ORIGINAL SCIENTIFIC PAPER

CROATICA CHEMICA ACTA

Croat. Chem. Acta **2018**, *91*(2), 153–162
Published online: June 13, 2018
DOI: 10.5562/cca3345

HKD 1926

Crystal Structure of *S*-adenosyl-L-homocysteine Hydrolase from *Cytophaga hutchinsonii*, a Case of Combination of Crystallographic and Non-crystallographic Symmetry

Justyna Czyrko,[1] Mariusz Jaskolski,[2,3] Krzysztof Brzezinski[1,*]

[1] Laboratory of Biochemistry and Structural Biology, Institute of Chemistry, University of Bialystok, Poland
[2] Center for Biocrystallographic Research, Institute of Bioorganic Chemistry, Polish Academy of Sciences, Poznan, Poland
[3] Department of Crystallography, Faculty of Chemistry, A. Mickiewicz University, Poznań, Poland
* Corresponding author's e-mail address: k.brzezinski@uwb.edu.pl

RECEIVED: April 16, 2018 * REVISED: May 6, 2018 * ACCEPTED: May 7, 2018

THIS PAPER IS DEDICATED TO DR. BISERKA KOJIĆ-PRODIĆ ON THE OCCASION OF HER 80TH BIRTHDAY

Abstract: The majority of living organisms utilize *S*-adenosyl-L-homocysteine hydrolase (SAHase) as a key regulator of cellular methylation reactions. The unusual evolution history of SAHase genes is reflected in the phylogeny of these proteins, which are grouped into two major domains: mainly archaeal and eukaryotic/bacterial. Such a phylogeny is in contradiction to the three-domain topology of the tree of life, commonly based on 16S rRNA sequences. Within the latter domain, SAHases are classified as eukaryotic-only or bacterial-only clades depending on their origin and sequence peculiarities. A rare exception in this classification is SAHase from a cellulose-utilizing soil bacterium *Cytophaga hutchinsonii* (ChSAHase), as the phylogenetic analyses indicate that ChSAHase belongs to the animal clade. Here, the $P2_12_12$ crystal structure of recombinant ChSAHase in ternary complex with the oxidized form of the NAD^+ cofactor and a reaction product/substrate (adenosine) is presented. Additionally, a sodium cation was identified in close proximity of the active site. The crystal contains two translational NCS-related intimate dimers of ChSAHase subunits in the asymmetric unit. Two complete tetrameric enzyme molecules are generated from these dimers within the crystal lattice through the operation of crystallographic twofold axes in the *z* direction.

Keywords: cellular methylation, *S*-adenosyl-L-homocysteine (SAH), *S*-adenosyl-L-methionine (SAM), cellulose degradation, X-ray crystallography, crystallographic symmetry, non-crystallographic symmetry (NCS), translational non-crystallographic symmetry (tNCS).

INTRODUCTION

S-ADENOSYL-L-METHIONINE (SAM) is the most common donor of methyl group in cellular methylation of a wide range of small- and macromolecular substrates.[1] During the methyl-group transfer, SAM is converted to *S*-adenosyl-L-homocysteine (SAH), which is a strong, negative-feedback inhibitor of SAM-dependent methyl-transferases and must be therefore efficiently removed. *S*-adenosyl-L-homocysteine hydrolase (SAHase) serves this purpose by catalyzing the reversible decomposition of SAH to adenosine (Ado) and L-homocysteine (Hcy). The equilibrium of this reaction is shifted far into the direction of SAH synthesis. Moreover, the activity of SAHase is inhibited by adenosine, which is a product of the hydrolysis reaction.[2,3] However, under physiological conditions, Ado and Hcy are rapidly removed from the environment and the net result is SAH hydrolysis.

SAHases usually function as 222-symmetric homotetramers,[4–11] or sometimes as homodimers.[3,12] Each subunit of the enzyme contains a tightly but non-covalently bound nicotinamide adenine dinucleotide cofactor in its oxidized form, NAD^+. Each monomer is comprised of two large domains, namely the substrate- and cofactor-binding domains, which are separated by a deep interdomain cleft. Additionally, each subunit contains a

This work is licensed under a Creative Commons Attribution 4.0 International License.

small C-terminal domain that plays a role in cofactor binding and protein oligomerization. The two principal domains (i.e., the substrate- and cofactor-binding domains) of the SAHase subunit are connected by two linker regions, folded as α-helical segments. During the catalytic cycle the enzyme oscillates between two conformational states: open (when ligand-free) and closed (ligand-bound). The open-closed movement of the domains is hinged upon the linker regions, which act like torsion-retorsion springs. The substrate/product delivery to/from the active site is regulated by a pair of highly conserved His-Phe residues, which function as a molecular gate.[3,7,8] Depending on the conformation of the gate, the entrance to the substrate-pocket access channel can be open or shut. Additionally, in the closed conformation, the enzyme coordinates a monovalent cation in close proximity of one of the hinge regions and of the active site area.

SAHase genes are present in the majority of (but not all) simple and complex organisms, including prokaryotic and eukaryotic microorganism, as well as plants and animals. However, they have evolved in an unusual way, and therefore the phylogeny of these enzymes is in contradiction to the three-domain topology of the tree of life, commonly based on 16S rRNA sequences.[13] In the phylogenetic analyses, SAHases are grouped into two major families, containing mainly archaeal or mainly eukaryotic/bacterial enzymes. Within the latter family, SAHases are classified depending on their origin and form, as eukaryotic-only or bacterial-only clades. A rare exception in this classification is SAHase from *Cytophaga hutchinsonii* (ChSAHase), a cellulose-utilizing soil bacterium, as in phylogenetic sequence analyses it is grouped within the animal clade, which suggests a late event of horizontal gene transfer.

In the present study, we have determined the crystal structure of the recombinant ChSAHase enzyme. The structure shows not only the enzyme complexed with one of the products of its hydrolytic reaction (adenosine), but also presents a case of a combination of crystallographic and non-crystallographic (NCS) symmetry. Although the asymmetric unit of the ChSAHase crystal contains indeed four subunits of the enzyme, they do not form one functional tetrameric unit. Instead, they are assembled into two dimers, located at two different crystallographic twofold axes, whose operation recreates two tetramers that are related by non-crystallographic translation (tNCS).

RESULTS AND DISCUSSION

Preparation and Crystallization of Recombinant ChSAHase

The expression and purification procedure was adjusted in order to obtain active, pure and homogeneous ChSAHase samples. Due to the fact that ChSAHase has a tendency to precipitate suddenly at higher concentrations, is was important to keep all the enzyme solutions at concentrations below 8 mg/mL. A similar effect of protein concentration on its stability in solution was observed for plant SAHase from yellow lupine.[3,14] Typical yields of ChSAHase were 10 mg of pure enzyme from 1 liter of expression culture. The effects of protein concentration and crystallization drop volume were investigated for optimization of the crystallization process. The best, diffraction-quality crystals were obtained using the hanging-drop vapor-diffusion method by mixing 2.5 μL of protein solution at 7.5 mg/mL, preincubated at 1:13 molar ratio with adenosine, with 2.5 μL of reservoir solution containing 15 % (*w*/*v*) PEG 8000 and 0.5 M Li_2SO_4. Under the optimized conditions, diffraction-quality crystals grew within ten days. The crystals are orthorhombic, space group $P2_12_12$ with unit cell parameters a = 96.28, b = 102.44, and c = 188.92 Å. The Matthews coefficient[15] was consistent with four protein chains of this tetrameric enzyme in the asymmetric unit (V_M = 2.43 Å^3/Da, solvent content 49.4 %). The native Patterson function showed a strong non-origin peak with 47 % of the origin peak height and located at 0, 0.5, 0.424, indicating translational non-crystallographic symmetry (tNCS) with a translation vector of ≈95 Å (Figure 1).

Determination of the Oligomerization State

SAHases are typically active as homotetramers. Recombinant ChSAHase is not an exception in this respect, as confirmed by ultrafiltration and SEC-FPLC (Figures 2A, 2B). For the enzyme concentration steps, we used ultracentrifugation membranes with 100 kDa cutoff and no protein was detected in the supernatant. This experiment clearly indicated that ChSAHase does not exist as a monomer (48 kDa) or dimer (96 kDa) in solution. The last step of protein purification was carried out using size exclusion chromatography (SEC). In this experiment, the recombinant enzyme was eluted in fractions corresponding to molecular mass of ≈200 kDa, indicating again the tetrameric state of ChSAHase (192 kDa).

Enzymatic Studies

Enzymatic activity assays with recombinant ChSAHase were performed in the direction of SAH hydrolysis and the following kinetic parameters were determined: the catalytic rate (k_{cat}) of the reaction is 0.042 ± 0.003 s^{-1}, substrate affinity (K_M) is 15.2 ± 1.6 μM, and the maximum velocity (V_{max}) is 2.60 ± 0.15 μM s^{-1}. The results of the kinetic analysis are shown in Figure 3.

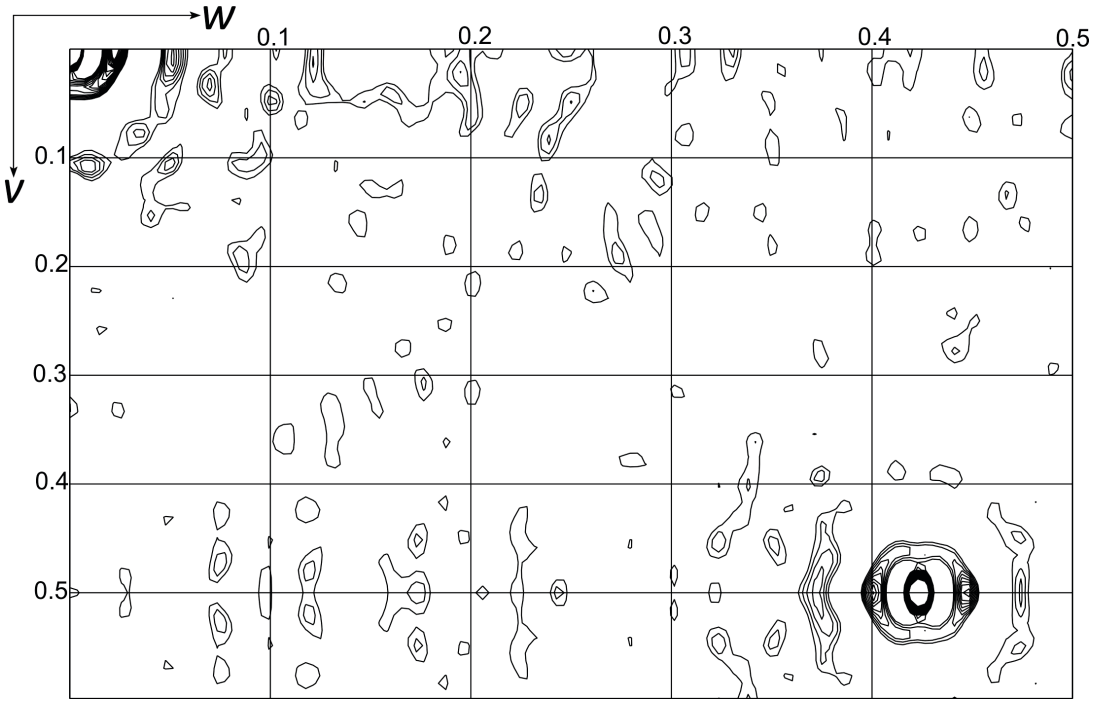

Figure 1. Section $u = 0$ of native Patterson function reveals a very significant non-origin peak at 0, 0.5, 0.424 which indicates the presence of tNCS corresponding to a translational vector of ≈95 Å.

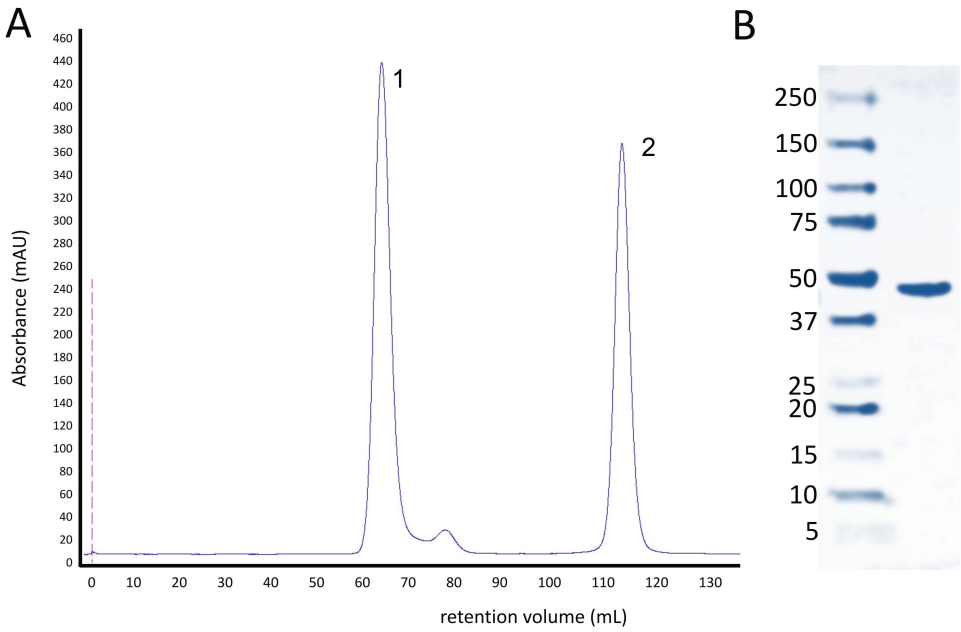

Figure 2. Purification and initial characterization of ChSAHase samples. (A) The final size exclusion chromatographic purification step recorded at 280 nm. Peak 1 corresponds to the tetrameric form of ChSAHase with the approximate molecular mass of ≈200 kDa, whereas peak 2 contains excess of the NAD^+ cofactor used for saturation of the apo form of the enzyme. (B) Chromatographic peak 1 fractions analyzed by SDS-PAGE (right lane) to confirm the correct size of the monomer of the recombinant ChSAHase protein. Molecular mass markers are shown in the left lane.

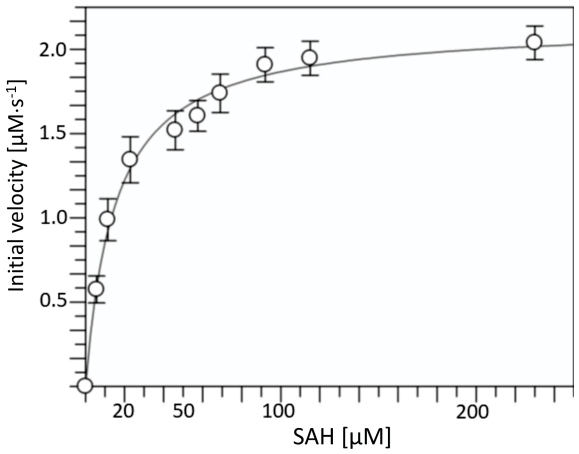

Figure 3. Kinetic analysis of recombinant ChSAHase determined using variable concentrations (from 0 to 230 μM) of *S*-adenosyl-L-homocysteine (SAH) as a substrate. Conversion of Hcy to Hcy-TNB was monitored spectrophotometrically at 412 nm. Initial velocities (in μM s^{-1}) were estimated from the linear region of the recorded curve. The values were obtained as averages of two replicates, bars represent standard error of the mean values (SEM).

Overall Structure of ChSAHase

ChSAHase crystalizes in space group $P2_12_12$ with two tNCS-related intimate dimers (labeled AB and CD) in the asymmetric unit (Figure 4). The conformation of the dimers is virtually identical, as illustrated by the r.m.s. deviation of 0.18 Å for the superposition of their 863 Cα atoms. Also the superposition of the individual subunits in each dimer is characterized by a similar r.m.s.d. value, at a rotation of ≈179.7° in each case, indicating a nearly perfect non-crystallographic symmetry of the intimate dimers. Each subunit, comprised of 435 amino acid residues, with a molecular mass of about 48 kDa, binds one adenosine (Ado, substrate or product) molecule and one NAD^+ (cofactor) molecule, as well as one sodium cation in the active site area. The structural organization of the subunit is similar to other SAHases and is shown in Figure 5. The fold consists of two large, well-separated main domains, the substrate-binding domain (residues 1–183 and 361–388) and the cofactor-binding domain (residues 196–355), plus an additional, small C-terminal dimerization domain (389–435). In the present crystal structure, each ChSAHase subunit adopts an adenosine-induced closed conformation. The precise location of the interdomain hinge regions is

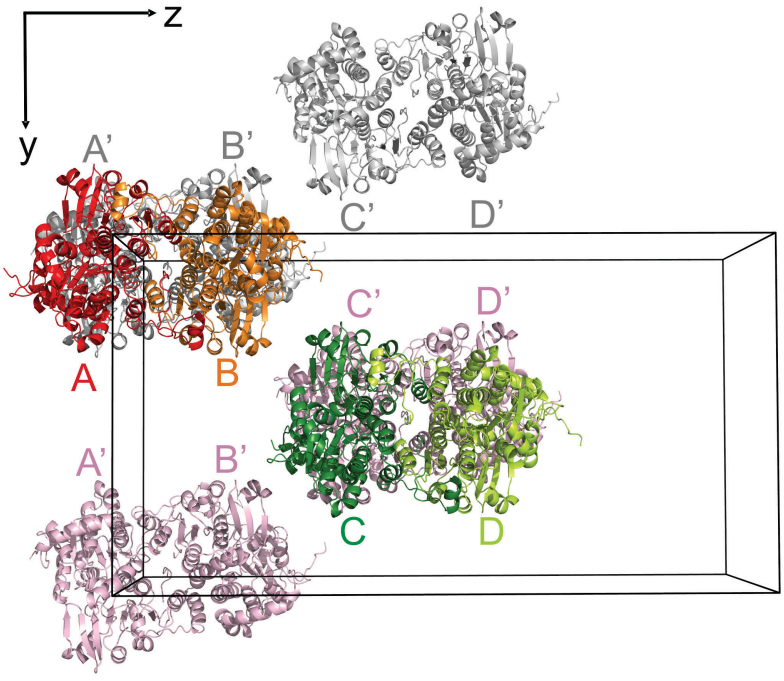

Figure 4. The two independent tNCS-related intimate dimers of ChSAHase forming the asymmetric part of the unit cell (outline), shown in a view along the *x* axis using ribbon representations colored red/orange (AB) and green/lime (CD). The two complete ChSAHase homotetramers are generated within the crystal lattice through the operation of crystallographic twofold axes along the *z* direction. Symmetry-related molecules A'B' and C'D' generated by crystallographic twofold axes at 0, 0 and 0, 0.5 are shown in gray and light pink, respectively.

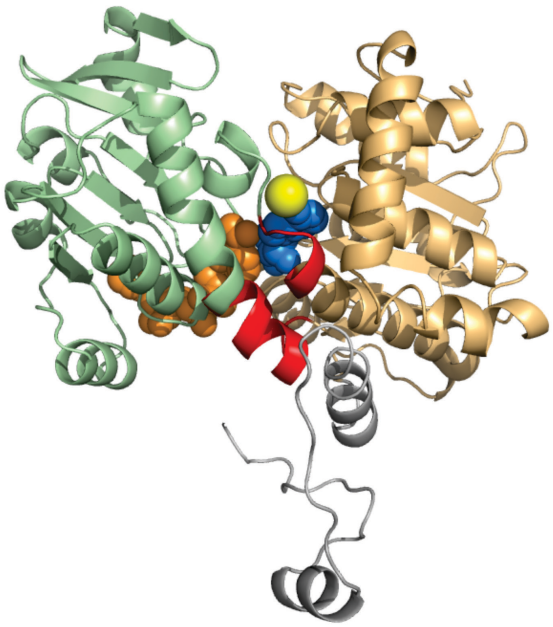

Figure 5. A ribbon diagram presenting the structure of one subunit (A) of ChSAHase in the closed conformation with the domains color-coded as follows: the substrate-binding domain (residues 1–183 and 361–388) is shown in light orange, the cofactor binding domain (residues 196–355) is shown in green, and the C-terminal domain (residues 389–435) is shown in gray. The two interdomain hinges (residues 184–195 and 356–360) linking the substrate and cofactor domains are shown in red. The NAD^+ cofactor (orange), adenosine (blue) and sodium cation (yellow) are shown in space-filling representation.

usually established by comparison of the open and closed conformations. Since this is not possible for ChSAHase, its linker segments (D184–K195 and H356–V360) were demarcated by sequence alignment with another bacterial SAHase, from *Bradyrhizobium elkanii*.[8,16]

A striking difference between the two tNCS-related intimate dimers AB and CD is visible in their mobility. The AB dimer is less flexible with the mean ADP (atomic displacement parameter) for main-chain atoms of 32.1 $Å^2$. The corresponding mean ADP value for the CD dimer is higher, 53.7 $Å^2$ Additionally, in the structure of the CD dimer significantly more side-chains (95 *vs* 40 in AB) were modeled with partial occupancy because of poorly defined electron density, which is usually a hallmark of high mobility and disorder. Despite the higher mobility of the CD dimer, the electron density maps were of very good quality, allowing unambiguous tracing of the main chain of all subunits. The exceptions are the N-terminal segments of chains A (M1-D3) and C (M1-F5) as well as all the artifactual cloning tripeptides, which could not be modeled because of disorder.

Table 1. Polar interactions with the adenosine molecule bound in the active site of ChSAHase, with the corresponding donor-acceptor distances (Å) in parentheses. Amino acid residues from the substrate (*) and cofactor (#) binding domains, as well as the monovalent cation coordinating loop ($) are involved in ligand binding. The interactions in all four subunits are almost identical; therefore, the distances are listed only for subunit A

Protein atom	Adenosine atom
*T58 Oγ	N1 (2.79)
*Q60 Oε	N6 (2.98)
$H356 O	N6 (3.15)
$H356 N	N7 (2.90)
*E159 Oε2	O2′ (2.83)
#D193 Oδ2	O2′ (2.63)
*T160 Oγ	O3′ (2.84)
#K189 Nζ	O3′ (2.99)
*H56 Nε2	O5′ (2.96)
*D134 Oδ1	O5′ (2.70)
#H304 Nδ1	O5′ (2.62)

Within the crystal lattice, crystallographic symmetry generates two complete ChSAHase tetramers, ABA′B′ and CDC′D′, through the operation of two different twofold axes, both along the *z* direction (Figure 4). Since the structure of the ABA′B′ tetramer is more rigid and complete, it will be used for further descriptions and comparisons, unless stated otherwise.

Enzyme-ligand Interactions

The crystal structure of ChSAHase was determined for a ternary complex with Ado substrate/product and NAD^+ cofactor. These two ligands are present in all subunits and are located in the active site (Ado) or in the crevice between the substrate- and cofactor-binding domains (NAD^+). Their ligand binding modes are presented in Table 1 (Ado) and Table 2 (NAD^+), and in Figures 6A and 6B, respectively. Additionally, one sodium cation is found in each subunit in close proximity of the active site. Its coordination mode is presented in Table 3 and Figure 6C. SAHases are highly conserved proteins, therefore it is not surprising that their interactions with both ligands, as well as with the monovalent cation are very similar among SAHases of various origin.[3,4,6–9,11,16]

The Mode of Adenosine Binding

The substrate-binding site of SAHases is formed by highly conserved amino acid residues. Therefore, the binding mode of Ado is similar to those observed in SAHases of various origin complexed with adenosine or its analogs. The amino acid residues involved in Ado binding are contributed by the two principal domains (Figure 6A). The

Table 2. Polar interactions with the NAD^+ molecule bound in the cofactor binding site of ChSAHase with the corresponding donor-acceptor distances (Å) in parentheses. Amino acid residues from the substrate (*) and cofactor (#) binding domains, as well as the C-terminal oligomerization domain from the adjacent subunit (@) are involved in cofactor binding. The interactions in all subunits are almost identical; therefore, the distances are listed only for subunit A and the adjacent subunit B

Protein atom	NAD^+ atom
*T160 Oγ	O2D (2.69)
*T161 Oγ	O1N (2.78)
*T162 Oγ	O3D (2.66)
*T162 N	O2D (3.17)
#N194 Nδ2	O1N (2.92)
#N227 N	O2N (2.90)
#E246 Oε1	O3B (2.48)
#E246 Oε2	O2B (2.72)
#N281 Nδ2	N7A (2.97)
#I302 O	N7N (2.93)
#H304 N	O3D (2.88)
#N349 Oδ1	N7N (3.08)
#N349 Nδ2	O7N (2.96)
@K429 Nζ	O2B (3.04)
@K429 Nζ	O3B (2.97)
@Y433 Oη	O2A (2.60)

purine ring is anchored in the binding site by several hydrogen bonds. The N6 atom is a donor in two hydrogen bonds, to the carbonyl group of H356 and the side-chain oxygen atom of Q60. It is of note that the latter residue is located in close proximity of the Na^+ ion . The main-chain N atom of H356 and the side-chain O atom of T58 are involved in hydrogen bonding with the N7 and N1 atoms, respectively. Additionally, the side chains of L350 and M361 constrict the binding cavity and stabilize the position of the ligand through, respectively, C–H···π and hydrophobic interactions with the purine ring. The O2' hydroxyl group of the ribose moiety interacts with the side chain oxygen atoms of E159 and D193. Additionally, the side chains of T160 and K189 form hydrogen bonds with the O3' atom. Finally, the carboxylate group of D134 and the side chains of H56 and H304 form a network of interactions with the ribose O5' atom. The latter residue is an element of the molecular gate formed by a tandem of the highly conserved H304-F305 residues which restrict access to the active site from the solvent region. In the present ChSAHase the molecular gate is in the shut state in all subunits.

The Mode of NAD^+ Binding

One NAD^+ cofactor molecule is found in each subunit of the ChSAHase model. It is located in the crevice between the two major domains and its binding mode, presented in Figure 6B, is very similar to that observed in other SAHases.

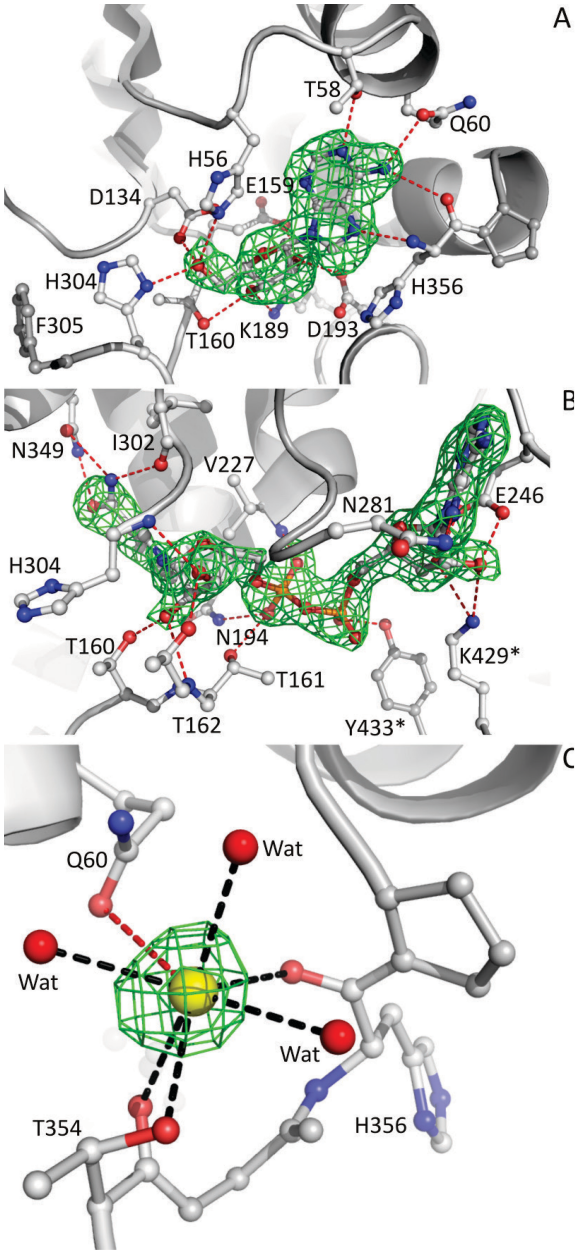

Figure 6. The modes of (A) adenosine, (B) NAD^+ cofactor, and (C) Na^+ cation binding in the area of the ChSAHase active site (shown for subunit A). Possible polar interactions are indicated by red dash lines, and the coordination bonds around the Na^+ cation (yellow sphere) as black dash lines. Water molecules are depicted as red spheres. Two amino acid residues from the adjacent subunit B (K429 and Y433) are marked with a star. The mF_o-DF_c OMIT difference electron density maps are contoured at 2.5σ (adenosine) or 3.0σ (NAD^+ and Na^+).

Table 3. Details of Na^+ ion coordination near the active site of ChSAHase with the corresponding cation-ligand distances (Å) listed for all chains (A–D)

Ligand atom:	T354 O	T354 Oγ	H356 O	Wat1	Wat2	Wat3
A	2.88	2.84	2.94	2.87	2.95	2.96
B	2.88	2.95	2.88	2.80	2.81	2.98
C	3.06	3.01	2.95	2.83	2.85	2.92
D	2.94	2.91	3.00	2.79	2.86	3.14

In the present structure, amino acid residues from both the cofactor- and substrate-binding domains are involved in hydrogen-bonding interactions with the NAD^+ molecule. Additionally, two residues from the C-terminal oligomerization domain from the adjacent subunit of the intimate dimer also participate in polar interactions with the cofactor. These interactions engage the main- and side-chain atoms of T160 (Oγ···O2D), T161 (Oγ···O2N) and T162 (N···O2D and Oγ···O3D) from the substrate-binding domain; of N194 (Nδ2···O2N), N227 (N···O1N), E246 (Oε1···O2B and Oε2···O3B), N281 (Nδ2···N7A), I302(O···N7N), H304 (N···O3D) and N349 (Nδ2···O7N and Oδ1···N7N) from the cofactor-binding domain; as well as K429 (Nζ···O2B and Nζ···O3B) and Y433 (Oη···O2A) from the adjacent C-terminal domain. The adenine moiety of the cofactor is sandwiched in a narrow cavity, restricted by the side chains of I247 and T279 which form vise-type C–H···π interactions with the purine ring. Additionally, seven water molecules participates in polar interactions with the cofactor molecule.

The Monovalent Cation Coordinated by ChSAHase

In the model of ChSAHase, all subunits exist in the closed conformation, with the substrate and cofactor domains clasped over the Ado substrate/product. In addition to the Ado molecule, each subunit coordinates a sodium cation in the substrate binding area. The Na^+ cation is found in the monovalent cation coordinating loop (T354–S356) in close proximity of the purine ring of the nucleoside, but it does not interact with the ligand directly. The coordination sphere of the sodium cation is a distorted octahedron formed by two main-chain carbonyl oxygen atoms provided by the T354 and H356 residues, as well as by the side-chain oxygen atom of T354. Finally, three water molecules complete the Na^+ coordination sphere. It is of note that the side chain oxygen atom of the Q60 residue located close to the sodium cation is involved in a cation-dipole interaction (Figure 6C). The Q60 residue is also involved in adenosine binding. A very similar coordination geometry of the Na^+ cation was observed in the crystal structures of other sodium-containing SAHases.[3,6,7,16]

Crystal Packing of ChSAHase

Although the asymmetric unit contains four subunits of ChSAHase, they are assembled into two unrelated dimers. The dimers are located at two different twofold axes along the *z* direction: AB at 0, 0 and CD at 0, ½, which generate from each of them a full 222-symmetric tetrameric molecule possessing both crystallographic and non-crystallographic symmetry. The two dimers selected in the asymmetric unit (AB and CD) are of the same type within the 222-symmetric homotetramer, i.e., they correspond to the so-called intimate dimers, which are mutually hooked into a tight structure by swapping of the C-terminal dimerization domains. It is interesting to note that the dimerization domain of subunit A participates in the formation of the cofactor binding site of subunit B and vice versa, and the same is of course true of the CD dimer.

In addition to the translation of $\Delta y = ½$ connected with the location of the point symmetry elements, the AB and CD dimers are also related by a translation of ≈80 Å along the *z* direction, which is equal to ≈0.42 of the c parameter of the unit cell. This translational non-crystallographic symmetry is clearly visible in the Patterson map (Figure 1), in which the highest non-origin peak (47 % of the origin) is located at 0, 0.5, 0.424. The combined AB-to-CD translation is equal to ≈95 Å and is coupled with a rotation of ≈1°, making this NCS symmetry of essentially translational type.

The non-crystallographic dyads of the ABA'B' tetramer, obviously parallel to the *xy* plane, are rotated by 7.9° from the crystallographic screws, as calculated by *ALIGN*.[17] In this alignment, the pseudo twofold axis of the 222 molecular symmetry that operates within the intimate AB dimer is nearly parallel to the crystallographic [100] direction. Similarly, the non-crystallographic dyads of the CDC'D' tetramer are rotated by 9.4° from the crystallographic screws, with the pseudo dyad relating C and D nearly parallel to [100]. A view of the molecular packing of the ChSAHase crystal is shown in Figure 4.

METHODS

Cloning, Expression, and Purification of ChSAHase

The coding sequence of the *sahH* gene was amplified by PCR from genomic DNA of *Cytophaga hutchinsonii* strain ATCC 33406 with the following primers: 5'-TACTTCCAATC-CAATGCCATGGTAGACACATTTGTAAAGCACAAAGTAAAAG

and 5'-TTATCCACTTCCAATGTTATTAGTATCTGTATTCGTCG-TTTTTATATGGGC. Subsequently, the amplicon was cloned into the pMCSG57 expression vector using the ligation independent cloning reaction. The correctness of the clone was confirmed by sequencing. The construct carrying the coding sequence of ChSAHase was used for transformation of BL21-CodonPlus(DE3)®-RIPL *Escherichia coli* cells and expressed. Briefly, 10 mL of TB medium containing 34 μg/mL chloramphenicol and 100 μg/mL ampicillin were inoculated and grown overnight at 310 K and the culture was used for inoculation of 1 L of TB medium that was cultivated with appropriate antibiotics to an OD_{600} of 1.0. The temperature was decreased to 291 K and protein expression was induced with IPTG at a final concentration of 0.3 mM. The cells were harvested 15 hours after induction and flash-frozen in liquid nitrogen.

The cell pellet was resuspended in 250 mL of buffer A (20 mM imidazole, 500 mM NaCl, 20 mM Tris·HCl pH 8.0, 10 % glycerol) with the addition of 0.5 mM TCEP·HCl and 100 μg/mL lysozyme. Cells were disrupted by sonication on ice and centrifuged at 277 K for 20 minutes at 4500 rpm. The supernatant was loaded onto a HisTrap column equilibrated with 0.1 M $NiSO_4$. The protein was eluted with 50 mL buffer containing 200 mM imidazole, 500 mM NaCl, 20 mM Tris·HCl pH 8.0, 10 % glycerol, and 1 mM TCEP·HCl. TEV Protease was added at a final concentration of 0.1 mg/mL and the protein solution was extensively dialyzed against buffer A. After overnight incubation at 277 K, the solution was loaded onto a HisTrap column equilibrated with 0.1 M $NiSO_4$ and the protein was eluted with buffer A, subsequently exchanged for buffer B (100 mM NaCl, 25 mM Tris·HCl pH 8.0, 1 mM TCEP·HCl) *via* dialysis. Next, a modified procedure of Yuan *et al.*[18] was used for the preparation of the apo form of the enzyme. Briefly, a solution containing 10 mg of recombinant ChSAHase dissolved in 5 mL of buffer B was gradually mixed with 10 mL of saturated solution of $(NH_4)_2SO_4$ at pH 3.3, and then stored for 10 min on ice. The mixture was centrifuged and the precipitate was dissolved in 5 mL of buffer B. The enzyme was precipitated again as above and the pellet was washed with saturated neutral solution of $(NH_4)_2SO_4$. Finally, the precipitated apo ChSAHase was dissolved in 2 mL of buffer C (100 mM NaCl, 25 mM Tris·HCl pH 8.0) and subsequently NAD^+ was added to a final concentration of 2 mM. After 30 minutes of incubation on ice, the mixture was loaded onto a Superdex 200 (Pharmacia) gel filtration column pre-equilibrated with buffer D (150 mM NaCl, 25 mM Tris·HCl pH 8.0, 1 mM TCEP·HCl). The protein was eluted with buffer D as a tetramer. Fractions with ChSAHase were concentrated to 7.5 mg/mL using Amicon Ultra 100 ultracentrifugation filters and subsequently passed through 0.22 μm filtration membrane. For all the subsequent experiments, fresh protein solutions were always used.

The purified protein is extended at the N-terminus by a short tripeptide (SNA-) cloning artifact. SDS-PAGE analysis confirmed the molecular weight of the expressed protein (≈48 kDa). Ultracentrifugation using filters with 100 kDa cutoff as well as size exclusion chromatography confirmed the tetrameric oligomerization state of ChSAHase in solution.

Assays for SAHase Activity

Assays for ChSAHase activity were performed in the hydrolytic direction. Enzymatic reactions were monitored spectrophotometrically and the rate of L-homocysteine (Hcy) formation was measured by monitoring its reaction with 5,5'-dithiobis(2-nitrobenzoic acid) (DTNB). Assays were performed in 3 mL volume in a buffer containing 100 mM KCl and 25 mM HEPES·KOH pH 7.5. The buffer was supplemented with six units of adenosine deaminase, 100 μM DTNB, and 0.35 μM of ChSAHase. The reaction was initiated by the addition of *S*-adenosyl-L-homocysteine (SAH) at a final concentration from 5.75 to 230 μM. The conversion of Hcy to Hcy-TNB was carried out at 295 K. The reaction progress was measured for one minute and monitored at 412 nm using a Hitachi U-3900H spectrophotometer. Initial velocity parameters were estimated from the linear region of the recorded curve. The experimental data were analyzed with the *GraFit* 7.0 software (Erithacus) to obtain the following kinetic parameters of the enzymatic reactions: substrate affinity (K_M), activity (V_{max}), as well as the catalytic rate (k_{cat}). All measurements were performed in duplicates.

Crystallization and X-ray Data Collection

Protein solution (5 mg/mL, measured spectrophotometrically at 280 nm) in buffer D was incubated overnight with 2 mM adenosine (1:13 molar ratio) at 277 K. The mixture was used for screening for crystallization conditions with a sparse-matrix screen[19] from Molecular Dimensions (Structure Screen 1). Crystallization drops for the screening experiments were mixed from 0.6 μL of the protein solution and 0.6 μL of the reservoir solution. Initial crystals were obtained at 292 K from 15 % (*w*/*v*) PEG 8000 and 0.5 M Li_2SO_4 using the sitting-drop vapor-diffusion method. The crystallization conditions were tuned by adjusting the protein concentration and volume of the crystallization drop. The best crystals were obtained at protein concentration of 7.5 mg/mL. They were grown using the hanging-drop vapor-diffusion method by mixing 2.5 μL of a ChSAHase-Ado solution with 2.5 μL of precipitating solution on a siliconized coverslide and equilibrating the drop against 1.0 mL of the precipitant solution. Diffraction-quality crystals appeared within ten days.

X-Ray diffraction data were measured at the BESSY synchrotron beamline 14.1 of the Helmholtz-Zentrum

Table 4. Crystallographic data, data collection and structure refinement statistics. Values in parentheses are for the last resolution shell

Data collection and processing	
Beamline	BESSY 14.1
Wavelength (Å)	0.91841
Temperature (K)	100
Space group	$P2_12_12$
Unit-cell parameters (Å)	
a	96.28
b	102.44
c	188.92
Resolution (Å)	50.0 – 2.09 (2.21 – 2.09)
Mosaicity (°)	0.12
Completeness (%)	99.6 (98.9)
Multiplicity	4.5 (4.6)
$\langle I/\sigma(I)\rangle$	13.0 (2.4)
R_{merge}	0.090 (0.731)
Refinement statistics	
Working/test reflections	108795/2101
R/R_{free}	0.210/0.231
No. of atoms / <B> (Å^2)	
Overall	14484/42.8
Protein	13457/43.5
Ado	76/36.5
NAD^+	176/38.4
Water	751/31.3
PEG	7/56.2
PG4	13/69.7
Na^+ ions	4/34.5
R.m.s.d. from ideality	
bond lengths (Å)	0.012
bond angles (°)	1.56
Ramachandran statistics (%)	
Most favored regions	98
Allowed regions	2
PDB code	6GBN

Berlin (HZB). A single crystal was soaked for a few seconds in the reservoir solution supplemented with 15 % (*v*/*v*) PEG 400, and then vitrified in liquid nitrogen prior to X-ray data collection. The diffraction data extend to 2.09 Å and were autoprocessed with *XDSAPP*[20] which makes use of *XDS*[21] and the *CCP4* suite.[22] The final data set is characterized in Table 4.

Structure Solution, Refinement, and Validation

The native Patterson map (Figure 1) showed a high non-origin peak at 0, 0.5, 0.424, implicating the existence of non-crystallographic translation of ≈95 Å in the unit cell. A preliminary solution of the crystal structure obtained by molecular replacement with the application of *PHASER*[23] from the *CCP4* suite and using chain A of *H. sapiens* SAHase[24] as the search model (PDB entry 1LI4) confirmed that the crystal packing indeed included two independent ChSAHase dimers located at two different crystallographic twofold [001] axes, with an additional translation of ≈80 Å along *z*. This preliminary solution revealed that the crystallographic twofold symmetry was not involved in the generation of the unique intimate dimer at each location. In order to generate a consistent description of the asymmetric unit contents, the structure was solved again, this time using the intimate dimer of *H. sapiens* SAHase as the search model (PDB entry 1LI4, chain A and its symmetry-related counterpart). The *PHASER* program was run in this case in the translation search mode with a minimum length of the translational vector of 90 Å, as estimated from the Patterson function. (It should be noted that in variance with the present ChSAHase case, the intimate dimer of *H. sapiens* SAHase *is* generated by crystallographic twofold symmetry.) The final solution is described in space group $P2_12_12$ with two separate tNCS-related intimate dimers (AB and CD) in the asymmetric unit, from which two different crystallographic dyads along *z* (at 0, 0 for AB and at 0, ½ for CD) generate two complete ChSAHase homotetramers (ABA'B' and CDC'D'). Automatic model building was carried out with the online version of *ARP/wARP*.[25] Isotropic stereochemically-restrained structure-factor refinement was carried out in *REFMAC5*[26] with maximum-likelihood targets and with the inclusion of automatically generated local NCS restraints. After a few rounds of minimization, three TLS groups per protein chain, as suggested by the *TLSMD* server,[27] were included in the refinement procedure.[28] The placement of the model in the unit cell was standardized with the *ACHESYM* server.[29] The ligands were identified without ambiguity in mF_o-DF_c omit electron density maps phased with the contribution of the protein atoms only. The alkali cation binding sites were confirmed as Na^+ with *CheckMyMetal*.[30] Water molecules and other components of the buffer solution were added only when unambiguously confirmed by electron density maps. The *COOT* program[31] was used for manual modeling in electron density maps. The stereochemical quality of the model was assessed using the wwPDB validation pipeline.[32] Atomic coordinates and ADP parameters, as well as structure factors have been deposited in the Protein Data Bank (PDB) with the accession code 6GBN. Raw X-ray diffraction images for the crystal structure of the ChSAHase-NAD^+-Ado ternary complex have been deposited in the RepOD Repository at the Interdisciplinary Centre for Mathematical and Computational Modelling (ICM) of the University of Warsaw, Poland, with the Digital Object Identifier (DOI) doi:10.18150/repod.4000773, and are available for download to all interested researchers from http://dx.doi.org/10.18150/repod.4000773. The final refinement statistics are reported in Table 4.

Abbreviations. Ado, adenosine; ADP, atomic displacement parameter; ChSAHase, *S*-adenosyl-L-homocysteine hydrolase from *C. hutchinsonii*; Hcy, L-homocysteine; DTNB, 5,5'-dithiobis(2-nitrobenzoic acid); FPLC, fast protein liquid chromatography; HEPES, 4-(2-hydroxyethyl)-1-piperazine-ethanesulfonic acid; IPTG, isopropyl-β-D-thiogalactoside; NAD^+ oxidized form of nicotinamide adenine dinucleotide; NCS, non-crystallographic symmetry; PCR, polymerase chain reaction; SAH, *S*-adenosyl-L-homocysteine; SAHase, *S*-adenosyl-L-homocysteine hydrolase; SAM, *S*-adenosyl-L-methionine; SDS-PAGE, sodium dodecylsulfate-polyacrylamide gel electrophoresis; SEC, size exclusion chromatography; TB, terrific broth medium; TCEP, tris(2-carboxyethyl)phosphine; TEV, Tobacco Etch Virus; Tris, 2-amino-2-hydroxymethyl-propane-1,3-diol; TNB, 2-nitro-5-thiobenzoic acid.

Acknowledgment. Work supported in part by an OPUS grant No. 2013/09/B/NZ1/01880 from the Polish National Science Centre. The BioNanoTechno Center at the Institute of Chemistry, University of Bialystok was founded by the European Funds for Regional Development and the National Funds of the Ministry of Science and Higher Education, as part of the Operational Programme Development of Eastern Poland 2007–2013, project POPW.01.03.00-20-034/09-00. The research leading to these results received funding from the European Community's Seventh Framework Programme (FP7/2007–2013) under BioStruct-X (grant agreement N 283570). Measurements were carried out at the BL14.1 beamline at Helmholtz-Zentrum Berlin (HZB). The authors thank HZB for the allocation of synchrotron radiation beamtime.

REFERENCES

[1] H. H. Richards, P. K. Chiang, G. L. Cantoni, *J. Biol. Chem*. **1978**, *253*, 4476.
[2] P. K. Chiang, *Pharmacol. Ther*. **1998**, *77*, 115.
[3] K. Brzezinski, Z. Dauter, M. Jaskolski, *Acta Crystallogr. D* **2012**, *68*, 218.
[4] M. A. Turner, C. S. Yuan, R. T. Borchardt, M. S. Hershfield, G. D. Smith, P. L. Howell, *Nat. Struct. Biol*. **1998**, *5*, 369.
[5] Y. Hu, J. Komoto, Y. Huang, T. Gomi, H. Ogawa, Y. Takata, M. Fujioka, F. Takusagawa, *Biochemistry* **1999**, *38*, 8323.
[6] N. Tanaka, M. Nakanishi, Y. Kusakabe, K. Shiraiwa, S. Yabe, Y. Ito, Y. Kitade, K.T. Nakamura, *J. Mol. Biol*. **2004**, *343*, 1007.
[7] M. C. M. Reddy, G. Kuppan, N. D. Shetty, J. L. Owen, T. R. Ioerger, J. C. Sacchettini, *Protein Sci*. **2008**, *17*, 2134.
[8] T. Manszewski, K. Singh, B. Imiolczyk, M. Jaskolski, *Acta Crystallogr. D* **2015**, *71*, 2422.
[9] Y. Zheng, C. -C. Chen, T. -P. Ko, X. Xiao, Y. Yang, C. -H. Huang, G. Qian, W. Shao, R. -T. Guo, *J. Struct. Biol*. **2015**, *190*, 135.
[10] K. Brzezinski, J. Czyrko, J. Sliwiak, E. Nalewajko-Sieliwoniuk, M. Jaskolski, B. Nocek, Z. Dauter, *Int. J. Biol. Macromol*. **2017**, *104*, 584.
[11] Y. Kusakabe, M. Ishihara, T. Umeda, D. Kuroda, M. Nakanishi, Y. Kitade, H. Gouda, K. T. Nakamura, N. Tanaka, *Sci. Rep*. **2015**, *5*, 16641.
[12] A. Guranowski, J. Pawelkiewicz, *Eur. J. Biochem*. **1977**, *80*, 517.
[13] T. Stepkowski, K. Brzeziński, A. B. Legocki, M. Jaskólski, G. Béna, *Mol. Phylogenet. Evol*. **2005**, *34*, 15.
[14] K. Brzezinski, G. Bujacz, M. Jaskolski, *Acta Crystallogr. F* **2008**, *64*, 671.
[15] B. W. Matthews, *J. Mol. Biol*. **1968**, *33*, 491.
[16] T. Manszewski, K. Szpotkowski, M. Jaskolski, *IUCrJ* **2017**, *4*, 271.
[17] G. E. Cohen, *J. Appl. Crystallogr*. **1997**, *30*, 1160.
[18] C. S. Yuan, J. Yeh, S. Liu, R. T. Borchardt, *J. Biol. Chem*. **1993**, *268*, 17030.
[19] J. Jancarik, S. H. Kim, *J. Appl. Crystallogr*. **1991**, *24*, 409.
[20] K. M. Sparta, M. Krug, U. Heinemann, U. Mueller, M. S. Weiss, *J. Appl. Crystallogr*. **2016**, *49*, 1085.
[21] W. Kabsch, *Acta Crystallogr. D 2010*, **66**, 125.
[22] M. D. Winn, C. C. Ballard, K. D. Cowtan, E. J. Dodson, P. Emsley, P. R. Evans, R. M. Keegan, E. B. Krissinel, A. G. W. Leslie, A. McCoy, S. J. McNicholas, G. N. Murshudov, N. S. Pannu, E. A. Potterton, H. R. Powell, R. J. Read, A. Vagin, K. S. Wilson, *Acta Crystallogr. D* **2011**, *67*, 235.
[23] A. J. McCoy, R. W. Grosse-Kunstleve, P. D. Adams, M. D. Winn, L. C. Storoni, R. J. Read, *J. Appl. Crystallogr*. **2007**, *40*, 658.
[24] X. Yang, Y. Hu, D. H. Yin, M. A. Turner, M. Wang, R. T. Borchardt, P. L. Howell, K. Kuczera, R. L. Schowen, *Biochemistry* **2003**, *42*, 1900.
[25] G. Langer, S. X. Cohen, V. S. Lamzin, A. Perrakis, *Nat. Protoc*. **2008**, *3*, 1171.
[26] G. N. Murshudov, P. Skubák, A. A. Lebedev, N. S. Pannu, R. A. Steiner, R. A. Nicholls, M. D. Winn, F. Long, A. A. Vagin, *Acta Crystallogr. D* **2011**, *67*, 355.
[27] J. Painter, E. A. Merritt, *J. Appl. Crystallogr*. **2006**, *39*, 109.
[28] M. D. Winn, M. N. Isupov, G. N. Murshudov, *Acta Crystallogr. D* **2001**, *57*, 122.
[29] M. Kowiel, M. Jaskolski, Z. Dauter, *Acta Crystallogr. D* **2014**, *70*, 3290.
[30] H. Zheng, D. R. Cooper, P. J. Porebski, I. G. Shabalin, K. B. Handing, W. Minor, *Acta Crystallogr. D* **2017**, *73*, 223.
[31] P. Emsley, B. Lohkamp, W. G. Scott, K. Cowtan, *Acta Crystallogr. D* **2010**, *66*, 486.
[32] H. Berman, K. Henrick, H. Nakamura, *Nat. Struct. Biol*. **2003**, *10*, 980.